International Journal of Engineering Research and Development
e- ISSN: 2278-067X, p-ISSN: 2278-800X, www.ijerd.com
Volume 21, Issue 6 (June 2025), PP 184-192

Optimization of a modern Jatropha-based Biodiesel Generator (GEBD) using the CPVTA-CAES Hybrid system

HARITHI BEN Daoud Ben Attoumane[1], PASERA Joanes Keneddy[2], DONA Victorien Bruno[3]

[1]PhD student, Laboratory of Applied Physics and Renewable Energies (LPADER), Ecole Doctorale Génie du Vivant et Modélisation (EDGVM), University of Mahajanga, Madagascar
[2]PhD student, Laboratory of Applied Physics and Renewable Energies (LPADER), Ecole Doctorale Génie du Vivant et Modélisation (EDGVM), University of Mahajanga, Madagascar
[3]Professor, Laboratory of Applied Physics and Renewable Energies (LPADER), Ecole Doctorale Génie du Vivant et Modélisation (EDGVM), University of Mahajanga, Madagascar
Corresponding Author : HARITHI BEN Daoud Ben Attoumane

ABSTRACT
The use of biofuel in internal combustion engines (gensets) is one of the alternatives to diesel (fossil fuel). Fossil diesel is a major producer of greenhouse gases, which are by no means negligible. On the other hand, biofuel is considered a clean, renewable solution comparable to pure diesel. Even if we have an alternative, biofuel, we also have the problem of the consumption of the Biodiesel Generator (GEBD). As a result, our work concerns both a contribution to the possibility of using jatropha as a fuel and an optimization of the jatropha-based GEBD through the valorization of compressed air. The latter was produced by a Photovoltaic Thermal Air Field (CPVTA), in order to achieve maximum reduction in biofuel (jatropha) consumption when using GEBD. Mathematical models were developed to demonstrate the savings achieved by the additional supercharging of compressed air stored as pneumatic energy (CAES) on the GEBD. The modelled parts of the modern engine are: air filter, compressor, heat exchanger, intake manifold, bio-engine combustion chamber and applied load. On this basis, we have also shown two equilibrium operations of the system: the case of GEBD without CAES and the case of GEBD with CAES. So, according to our simulated results, compressed air is a key asset in reducing the biofuel consumption of the bio unit, even by up to 60% at high loads.

Keywords : *Energy, Photovoltaic, Thermal, Storage, Pressure, Compressed air, Engine, Biofuel*

Date of Submission: 15-06-2025 Date of acceptance: 30-06-2025

I. INTRODUCTION

The use of Renewable Energies (RE) in Madagascar has become extremely important due to the recent rise in oil prices and the remoteness of certain sites from the JIRAMA networks. In the Boeny region (Mahajanga), known for its high solar irradiance, we use photovoltaic (PV) solar panels to harness this energy. However, the technique most commonly used to achieve good yields and autonomy is sometimes the hybridization of PVs with renewable and/or non-renewable sources such as diesel. Diesel power generation presents major environmental risks, such as contamination of ambient air and a considerable contribution to greenhouse gas (GHG) emissions. The latter is more than 11.2 million tonnes a year. Thus, biofuel remains an alternative to the GHG increases produced by diesel engines. The biofuel used in this study is based on jatropha from Madagascar, preheated to a 45% blend with diesel.

The aim of this article is to demonstrate the possibility of reducing biofuel consumption by using solar energy stored in the form of compressed air (CAES). In fact, the electrical energy produced by the thermal photovoltaic field feeds the load and at the same time is stored in the form of compressed air in a tank, in order to supercharge a modern Biodiesel Generator. The latter is a generator with a turbocharger. We've limited the CAES storage pressure to 70 bar, because biodiesel generators can't handle high pressures (Hussein, 2010). So there's no point in storing air at 200 bar (BEN, 2025) and lowering it to 6 bar for the biodiesel engine. In fact, this technology converts the chemical energy of jatropha mixed with diesel into mechanical energy on the crankshaft and electrical energy on the alternator shaft (Hussein Ibrahim et al., 2009). Mathematical models have been demonstrated to indicate the advantage that compressed air can have on GEBD fuel consumption. As a result, the jatropha-based biodiesel engine running with or without CAES has been modeled. We found that the air/fuel ratio decreased with increasing load for a GEBD without compressed air. The system was therefore optimized to achieve a constant air/fuel ratio that corresponds to the engine's maximum efficiency, thereby reducing biofuel consumption. The result is promising electricity production and reduced greenhouse gas emissions. Since the CO_2released during combustion will be re-stored in a plant the following season.

What's more, in the event of a solar shortage/low solar intensity, the CPVTA will not be able to meet electricity requirements. In this case, the GEBD motor will have to be switched on automatically to meet load requirements. As a result, stored pneumatic energy will be sent directly upstream of the turbocharger compressor to ensure optimum excess airflow, leading to fuel economy. Hence system optimization.

II. MATERIAL AND METHODS

Mathematical models of the system have been introduced to simulate our system. Figure 1 shows a schematic diagram of the model studied:

Figure1: System modeling

2.1 Architecture of the system studied

Our system consists of a field of Air Thermal Photovoltaic panels. This feeds a compressed-air storage system, featuring an electric motor, a reservoir strong enough to withstand high pressures (70 bar to 200 bar) and a modern biodiesel generator. Part of the CPVTA's electrical energy is sent directly to the load.

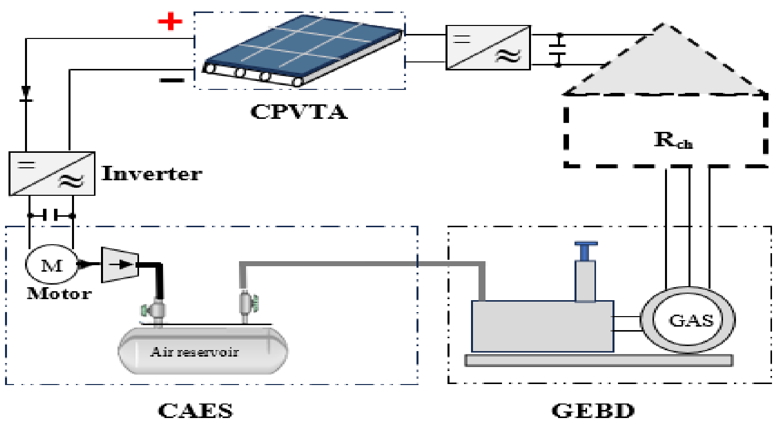

Figure2: System configuration (CPVTA-CAES-GEBD)

2.2 Global system modeling assumptions

Throughout this study, we will consider the following hypotheses (Sidiki et al, 2017; Bruno et al, 2019; Attoumane et al., 2024; Ibrahim, 2010):

- Air has the properties of a perfect gas (CPVTA-CAES-GEBD).
- Pressure losses in working fluids are neglected (CAES).
- The moisture content of the system is negligible (CAES).
- The kinetic and potential energies inside the CAES are negligible.
- Gravity is negligible in the compression and expansion stage.
- Modeling is carried out dynamically, but some components are treated statically, since heat accumulation and mass are not taken into account for these components (CAES).
- Compression and expansion are polytropic transformations.
- The dead volume of the compressor is negligible.
- The intake manifold is a thermodynamically open and adiabatic (GEBD) system.
- The exhaust manifold is polytropic (GEBD).
- Variations in heat capacities at constant volume and constant pressure with temperature are negligible (GEBD).

2.3 Electrical power generated by the CPVTA

To ensure the system's efficiency (CPVTA-CAES-GEBD), we have chosen the air PVT as the source of electrical power for air compression. Thus, the electrical power produced by the PVT field is given by the expression (Khaled, 2010):

$$P_{PVT} = P_s.\eta_{réf}.\alpha_{sil}^{-1}.\exp\left[\beta\left(T_{cel} - T_{réf}\right)\right] \tag{1}$$

$P_s = \tau_v.\alpha_{sil}.G.S$ represents the power absorbed by the solar cells.

G *et* S respectively represent the overall irradiance received on the plane and surface of the PVT field.

2.4 Energy required for compression

The energy required for compression has been determined from the work involved in transferring air from the compressor inlet to the outlet. Thus the total energy per unit mass of air passing through the multi-stage compressor (N stages), which is characterized by the same compression ratio in each compressor stage due to having a high efficiency, is (Sidiki et al., 2017; Attoumane et al., 2025) :

$$E_c\left(\tau_c\right) = \frac{N_c n_c}{n_c - 1} r T_1 \left(\tau_c^{\frac{n_c - 1}{N_c n_c}} - 1\right) \tag{2}$$

2.5 Compressed air tank volume

The air volume is expressed in terms of the maximum and minimum permissible pressures in the air motor, the desired autonomy and the maximum air flow rate to operate the motor (Ibrahim, 2010; Sidiki et al., 2017; Attoumane et al., 2025) :

$$V_{res} = \frac{P_a \dot{V}_{max} a}{P_{max\_MAC} - P_{min\_MAC}} \tag{3}$$

2.6 Energy stored in the reservoir per unit volume

The energy stored per unit volume depends on the reservoir pressure and the subsequent use (expansion) of the stored air (Houssen, 2010; Attoumane et al., 2025):

$$E_{st} = p_{st} \frac{k n_d N_d}{n_d - 1} \left(1 - \left(\frac{p_a}{p_{st}} \right)^{\frac{n_d - 1}{n_d N_d}} \right) \quad (4)$$

2.7 Modeling the biodiesel engine without CAES

Modern engines still feature a turbocharger, and we can model its components: air filter, compressor, heat exchanger, intake manifold, combustion chamber and applied load.

2.7.1 Air filter modeling

The air filter is modeled by the equations of pressure and temperature passing through it (Hussein, 2010):

$$P_{s\_filtre} = P_{stock} - k_{filtre} \frac{\dot{m}_{res}}{\rho_{air}} \quad (5)$$

$$T_{s\_filtre} = T_{e\_filtre} \left(\frac{P_{s\_filtre}}{P_{stock}} \right)^{\frac{\gamma}{\gamma - 1}} \quad (6)$$

k_{filtre} is the coefficient of singular pressure drop in the air filter.

2.7.2 Compressor modeling

The compressor is modelled by knowing the power consumed, the temperature and the pressure at the compressor outlet:

$$P_C = \dot{m}_C C_p T_{e\_C} \frac{1}{\eta_C} \left(\pi_C^{\frac{\gamma - 1}{\gamma}} - 1 \right) \quad (7)$$

$$T_{s\_C} = T_{e\_C} \left(1 + \frac{\pi_C^{\frac{\gamma - 1}{\gamma}} - 1}{\eta_C} \right) \quad (8)$$

$$P_{s\_C} = P_{e\_C} \pi_C$$

π_C and η_C are the compressor's compression ratio and isentropic efficiency, respectively.

2.7.3 Heat exchanger modeling

The heat exchanger cools the air leaving the turbocharger. Cooling takes place at constant pressure. In this case, the heat exchanger is modelled by the air temperature at the exchanger outlet (Hussein, 2010):

$$T_{s\_ech} = T_{s\_C} \left(1 - \eta_{ech} \right) + \eta_{ech} T_{air\_ref} \quad (9)$$

η_{ech} and T_{air_ref} are heat exchanger efficiency and cooling air temperature respectively.

2.7.4 Intake manifold modeling

The intake manifold is modeled by the amount of air admitted into the cylinder (Hussein, 2010):

$$\dot{m}_{e\_Bio} = \dot{m}_C = \eta_{v\_Bio} \cdot \left(\frac{C_{y\_Bio} . P_{e\_Bio}}{4\pi . r . T_{e\_Bio}} \omega_{Bio} \right) \quad (10)$$

η_{v_Bio} is the fill rate of the biodiesel engine, expressed by the expression (Gisinger, 2002) :

$$\eta_{v\_Bio} = \alpha_0 + \alpha_1 . \omega_{Bio} + \alpha_2 . \omega^2_{Bio} \quad (11)$$

ω_{Bio} is the rotation speed of the biodiesel engine.

α_0 , α_1 *et* α_2 are parameters derived from experimental data.

2.7.5 Engine combustion chamber

The power produced by the motor must match the total resistive power of the motor (Jensen et al, 1991):

$$P_{i\_Bio} = P_{diss\_Bio} \quad (12)$$

P_{i_Bio} is the power supplied by the motor (Jensen et al, 1991; Hussein, 2010):

$$P_{i\_Bio} = p_{ci} \eta_{i\_Bio} \dot{m}_{carb} \quad (13)$$

P_{diss_Bio} is the total resistive power of the motor and can be expressed as (Younes, 1993) :

$$P_{diss\_Bio} = \left(P_{mf\_Bio} \frac{C_{y\_Bio}}{4\pi} + C_{r\_Bio} \right) \omega_{Bio} \quad (14)$$

P_{mf_Bio} is the average friction loss pressure and is expressed by the formula (Hussein , 2010) :

$$P_{mf\_Bio} = 0,97 + 0,15 \left(\frac{N_{Bio}}{1000} \right) + 0,05 \left(\frac{N_{Bio}}{1000} \right)^2 \quad (15)$$

2.8 Modeling the biodiesel engine with CAES

The problem to be solved is the same as in a biodiesel engine without CAES. The difference, however, is in the fuel consumption of the engine, which must operate with an optimum air/fuel ratio $\lambda = \lambda_{optimal}$. In addition, the pressure at the compressor inlet is that of the compressed air leaving the CAES.

2.9 Motor efficiency

Because the biodiesel engine operates at constant speed, i.e. no time variations but changes from one speed to another that also varies according to the load applied to the engine and the air speed, the indicated engine efficiency is modeled by the following expression (Houssen, 2010):

$$\begin{cases} \eta_{i\_Bio} = a + b\lambda + c\lambda^2 \;\; si \;\; \lambda \geq \lambda_{stoc} \\ \eta_{i\_Bio} = \left(a + b\lambda + c\lambda^2 \right) . \dfrac{\lambda}{\lambda_{stoc}} \;\; si \;\; \lambda < \lambda_{stoc} \end{cases} \quad (16)$$

λ_{stoc} is the stoichiometric air/fuel ratio.

III. RESULTS

We used the same characteristics of the CPVTA/compressor and the same meteorological data from the Mahajanga site: 15°43' Sud (latitude), 46°19' Est (longitude), which we have already dealt with (Attoumane et al., 2024), for the simulations (under MATLAB). Page's model was used to estimate the site's mean annual global irradiance (Attoumane et al., 2024; Benhammou, 2010). In Mahajanga, the maximum average irradiance value is found in October (close to 1000 $W.m^{-2)}$, while it is very low in January at close to 700 $W.m^{(-2)}$ (Attoumane et al., 2024). Similarly for electricity production, for a PVT field surface area of around 50 m^2, maximum power reaches 4.1 kW (in October) and 2.8 kW in January (Attoumane et al., 2024). Inverter power conversion is around 98.5%. The choice of relevant parameters, influencing the system studied (CPVTA-CAES-GEBD) are set to supercharge a jatropha-based biofuel engine and for load requirements. Table 1 shows the limits and choices of some of the parameters used in this work.

Table 1: Limits of the parameters studied and proposed choice (Attoumane et al., 2024)

Parameter studied	Limit	Choice	Unit
PVT field area	Variable	50	m^2
PVT field power	Variable	3	kW
Maximum stored pressure	5 - 500	80	bars
Reservoir volume	Variable	100	L
Number of stages (Compressor)	1 - 5	3	-
Charging time (tank)	Variable	1.8	h
Discharge time (Reservoir)	Variable	1	h
Product power (GEBD)	Variable	12	kW
Indicated yield (GEBD)	Variable	40	%

3.1 Engine torque as a function of internal combustion engine speed

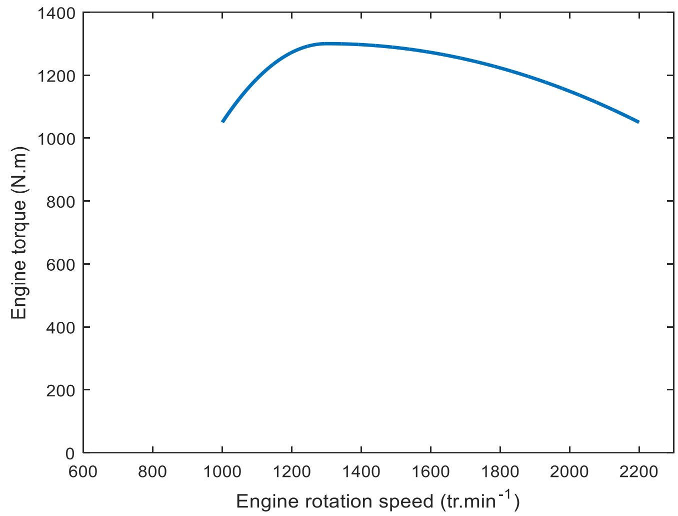

Figure3: Motor torque

Figure 3 shows how the speed of a stationary generator varies as a function of engine torque. At lower engine speeds up to 1400 rpm^{-1}, engine torque increases. This can increase up to 1300 N.m. On the other hand, for rotations from 1400 rpm^{-1}upwards, motor torque decreases. In this study, we set the motor torque at 1300 N.m with a motor speed of 1400 rpm^{-1}.

3.2 Air/fuel ratio as a function of engine torque

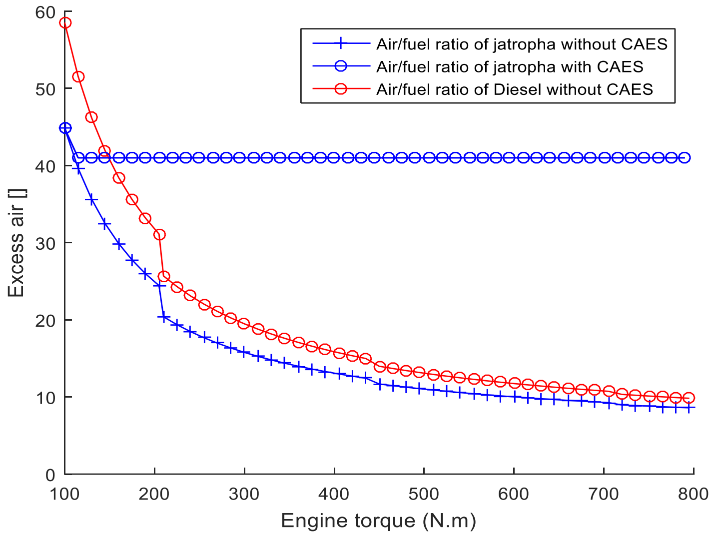

Figure4: Air/fuel ratio comparison

Figure 4 shows that excess air in an internal combustion engine decreases with increasing engine load. This leads to a drop in engine efficiency as fuel consumption increases. On the blue curve, which shows the evolution of the air/fuel ratio of jatropha without stored air, a torque of 100 N.m has an excess air of 45. This is sufficient for complete combustion of the jatropha. On the other hand, at high torque (800 N.m), the excess air is 10, resulting in unburnt biofuel. As a result, the engine may consume fuel due to incomplete jatropha combustion caused by insufficient air. However, with the presence of the CAES at the engine intake, we note that at smaller loads (below 130 N.m), the engine operates at a higher than optimal excess air $\left(\lambda_{optimal} = 42\right)$. This implies that, at this limit, we don't need additional air for the turbocharger. But with torques in excess of 130 N.m, the biodiesel engine can no longer ensure sufficient air quantity for optimum excess air. The engine will therefore run on the air reservoir stored by the CPVTA (green curve). The red curve shows a reference result for a diesel generator (Younes, 1993).

3.3 Fuel **consumption**

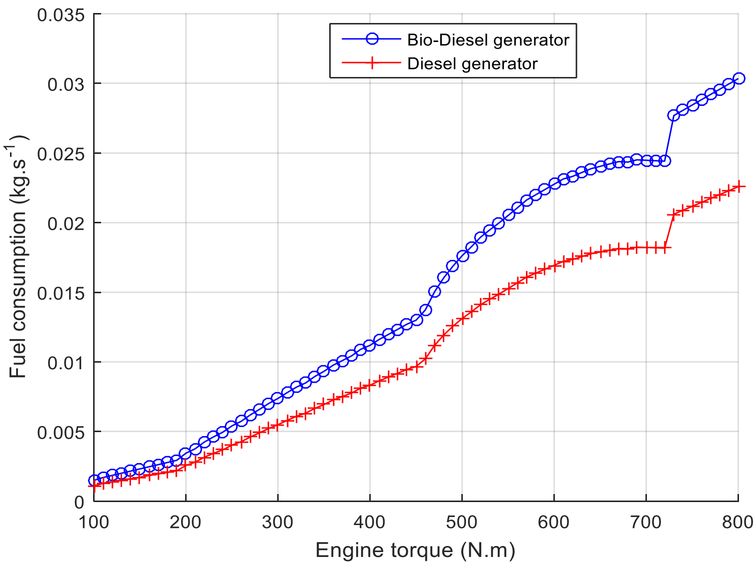

Figure 5: Comparison of fuel consumption ratio (jatropha/gasoil)

Figure 5 shows that fuel consumption increases with increasing engine load. The blue curve shows the consumption of the GEBD without CAES. With a load of 800 N.m, we need 0.03 kg.s^{-1}of jatropha. On the other hand, for the same load, we need a flow rate of 0.023 $kg.s^{-1}$ for diesel. This difference remains in the calorific value and ketone number of the two fuels (diesel > jatropha). Even with this difference in consumption, jatropha remains an alternative for diesel, because it is a renewable energy.

3.4 Fuel consumption with and without CAES

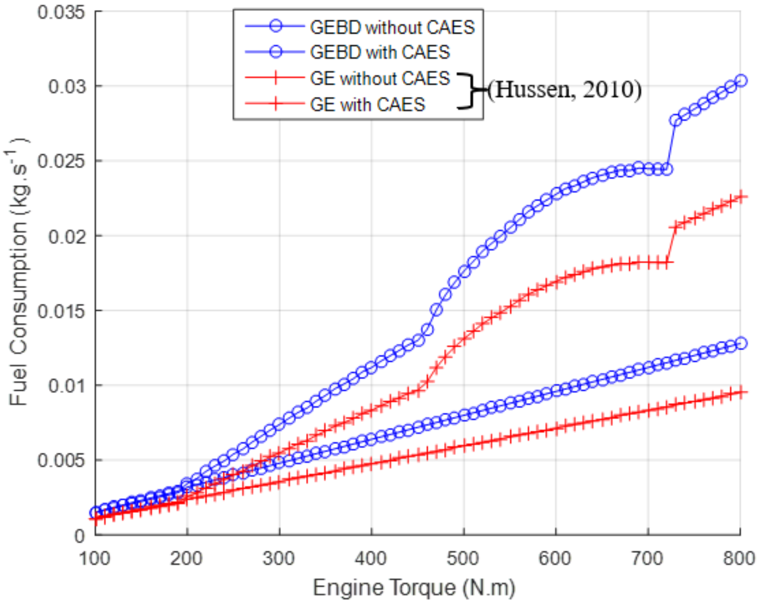

Figure6: Fuel consumption (Jatropha/Gasoil)

Figure 6 shows that CAES support (compressed air storage) has reduced engine fuel consumption. For jatropha, with a load of 800 N.m in the presence of compressed air, the biofuel flow rate is reduced to 0.013 $kg.s^{-1}$. And diesel, with the same load, is reduced to 0.0095 $kg.s^{-1}$.

3.5 Biodiesel and diesel generator efficiency

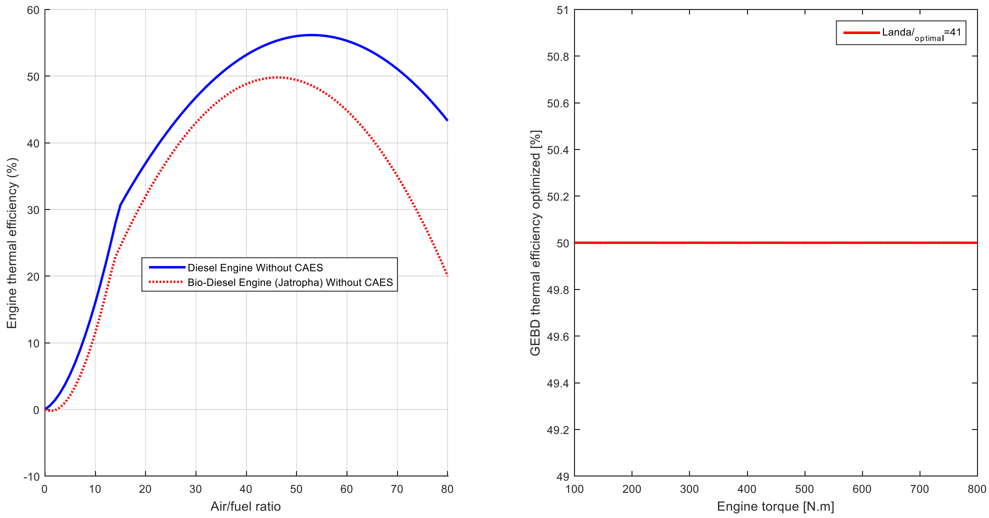

Figure 7: Indicated efficiency of the internal combustion engine

Figure 7 on the right shows that the efficiency of the stationary internal combustion engine increases with air/fuel ratios ranging from 0 to 42 for jatropha. It decreases with higher ratios than the optimum. For example, we record a maximum efficiency of 50% for an air/jatropha ratio of $(\lambda_{optimal} = 42)$. However, an atmospheric or turbocharged jatropha engine will not be able to achieve this efficiency without the support of additional compressed air. So, whatever the load applied to the engine (figure 8 left), CAES always stabilizes the air/fuel ratio at the optimum value. As a result, efficiency will be constant (50%) for all loads applied to the engine. We have presented the efficiency of diesel (blue curve) for reference of our results with those of (Hussein, 2010). We can see that the efficiency of diesel is slightly higher than that of jatropha. This is always explained by the calorific value of diesel, which is higher than that of jatropha.

IV. CONCLUSION

In conclusion, this study shows that it is possible to combine a CAES, powered by a CPVTA, with a jatropha-based engine in order to achieve total fuel savings through the use of additional compressed air. We would like to make it clear that the diesel genset results (Hussein, 2010; Younes, 1993) used in this work are taken as a reference for our simulated biodiesel genset results (GEBD-jatropha). The reason is that we don't yet have experimental results to validate our theoretical results for the biofuel (jatropha). So, until now, the scientific literature remains our point of reference.

However, as the biodiesel engine operates at constant speed, fuel economy, which is all the more important, is determined by the increase in engine load applied. Simulations have shown satisfactory solutions. For example, with a 4-litre engine running at a speed of 1400 rpm^{-1}at constant engine speed and a 100-litre air tank storing air at a pressure of 80 bar, we recorded an optimum air/fuel ratio ($\lambda = 42$). With this excess air, the GEBD operates at its maximum efficiency (50%) for all loads applied to the modern engine. In addition to its maximum efficiency, the support of compressed air also enables the GEBD to operate at a fuel economy of 60% for high loads. Thus, for a load of 800 N.m applied to the engine (without CAES), we have a flow rate (for jatropha) of 0.03 $kg.s^{-1}$. But in the presence of CAES, the flow rate decreases to 0.013 $kg.s^{-1}$. So the biodiesel generator (jatropha) is optimized by the gain of stored solar energy (CPVTA) in the form of compressed air.

The next logical step is to carry out an experiment on a jatropha-based biodiesel engine supercharged by a CAES running on CPVTA, in order to compare our simulated results with our own experimental results.

REFERENCES

[1]. HARITHI BEN D. B. A., Pasera J. K., and DONA V. B. 2024, Energy performance studies of a PVT-AIR system with CAES: influence of input parameters on the compression system, IJARIIE-ISSN(O)-2395-4396, Vol-10 Issue-4, pp. 67 - 74.

[2]. Hussein Ibrahim, Mariya Dimitrova, Adrian Ilinca, Jean Perron. 2009. Wind-diesel hybrid system with compressed air storage for electrification of an isolated telecommunication station. European Journal of Electrical Engineering, Volume 12/5-6, pp.701-731.

[3]. Hussein Ibrahim, (2010). Etude et conception d'un générateur hybride d'électricité de type éolien-diésel avec élément de stockage d'air comprimé, thesis, Université du Québec à Chicoutimi, Canada, June 2010

[4]. SIMPORE Sidiki, (2018). Modeling, simulation and optimization of a compressed air storage system coupled to a building and photovoltaic generation, Thesis. Université de la Réunion, France.

[5]. N. M. Jubeh and Y. S. H. Najjar, (2012). Green solution for power generation by adoption of adiabatic CAES system, Appl. Therm. Eng. vol. 44, p. 85 89.

[6]. N. M. Jubeh and Y. S. H. Najjar, (2012). Power augmentation with CAES (compressed air energy storage) by air injection or supercharging makes environment greener, Energy, vol. 38, no. 1, p. 228 235 .

[7]. Ilham rais and Hassan Mahmoudi, (2016). The control strategy for a hybrid wind photovoltaic system with compressed air storage element, 2nd International Conference on Electrical and Information Technologies ICEIT2016, (ICEIT), Tangiers, pp. 89-92.

[8]. TOUAFEK Khaled, 2010. Contribution à l'étude et à la conception d'un système énergétique utilisant des capteurs hybrides photovoltaïques thermiques, thesis, Ecole Normale Polytechnique ENP, Algeria.

[9]. Sidiki Simpore et al, 2017. Systeme de stockage à air comprimé couplé à un batiment et à une production photovoltaique en zone insulaire et tropicale : Etude de semsibilité parametrique, XIIIeme Colloque Interuniversitaire Franco-Québécois, CIFQ2017/ART-07-11, Thermique des systemes, Saint-Lo, France, LUSAC

[10]. Amina Benhammou, 2010. Optimisation d'un nouveau système de séchage solaire modulaire pour plantes aromatiques et médicinales, thesis, Université Abou Beker Belkaid, Algeria.

[11]. DONA Victorien Bruno and al, 2019. Estimate of photovoltaic energy production during the sunniest month in Mahajanga, IJARIIE-ISSN(O)-2395-4396, Vol-5 Issue-4, pp. 92 - 103.

[12]. HARITHI BEN Daoud Ben Attoumane and al, (2024). Energy storage in the form of compressed air with an air PVT field: Influence of input parameters on the air reservoir, IJARIIE-ISSN(O)-2395-4396, Vol-10 Issue-4, pp. 3096 - 3104.

[13]. Gissinger G, Le Port-Piat N, (2002). Controle-Commande de la voiture. Editions Hermes & Lavoisier.